Imaging nuclei by smashing them

Jiangyong Jia

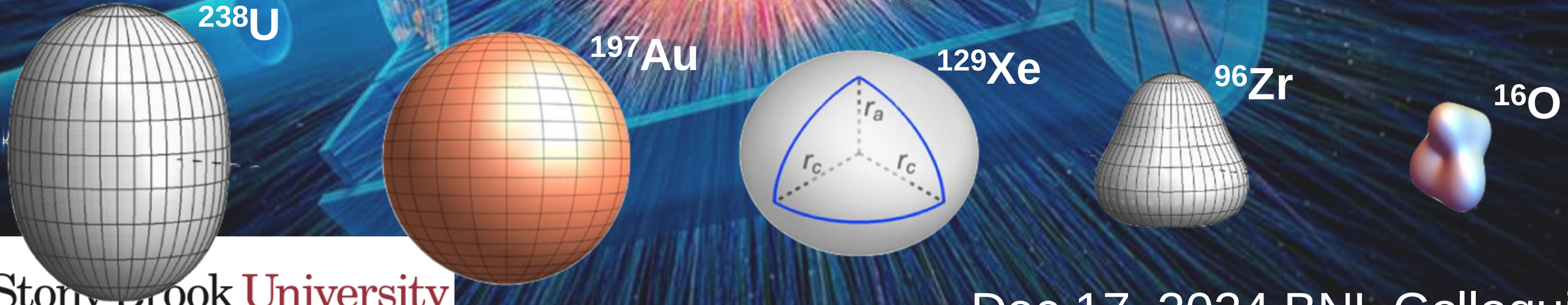

Stony Brook University

Dec 17, 2024 BNL Colloquium

Traditional imaging method

Coherent diffraction

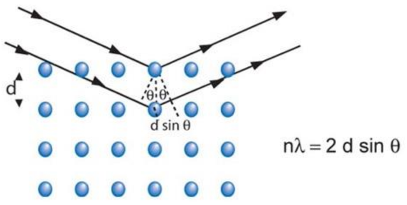

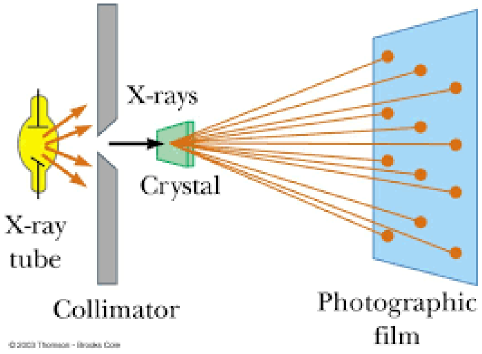

Inverse Fourier transform

$$\rho(xyz) = \frac{1}{V} \sum_{hkl\ -\infty}^{+\infty} |F(hkl)| \ . \ e^{-2\pi i[hx+ky+lz-\phi(hkl)]}$$

Amplitudes

Phases

Traditional imaging method

$$\gamma + \underset{\mathrm{Au}}{\mathrm{p}} \rightarrow \mathrm{J}/\psi + \underset{\mathrm{Au}}{\mathrm{p}}$$

Coherent diffraction

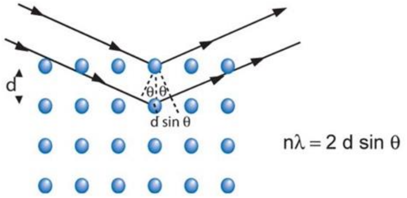

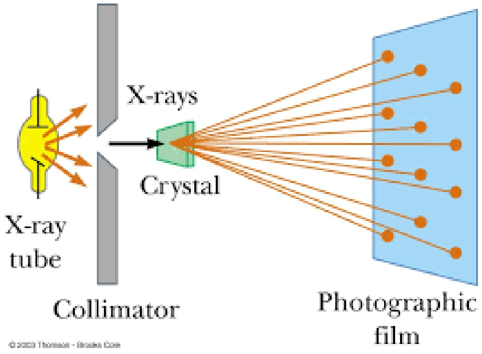

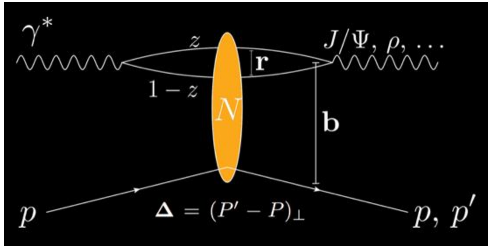

Inverse Fourier transform

Sensitive to the averaged structure of the p/Au

$$\rho(xyz) = \frac{1}{V}\sum_{hkl=-\infty}^{+\infty} \underbrace{|F(hkl)|}_{\text{Amplitudes}} \cdot e^{-2\pi i[hx+ky+lz-\underbrace{\phi(hkl)}_{\text{Phases}}]}$$

$$\frac{d\sigma^{\gamma^* p \rightarrow Vp}}{dt} = \frac{1}{16\pi}\left|\left\langle A^{\gamma^* p \rightarrow Vp}\left(x_P, Q^2, \vec{\Delta}\right)\right\rangle\right|^2$$

$$A \sim \int d^2b\, dz\, d^2r\, \psi^*\psi^V(\vec{r}, z, Q^2) e^{-i(\vec{b}-(\frac{1}{2}-z)\vec{r})\cdot\vec{\Delta}} N(\vec{r}, x, \vec{b})$$

Image taken before destruction

Imaging by smashing: some examples

Smashing a deformed droplet on surface

$$F = \nabla P$$

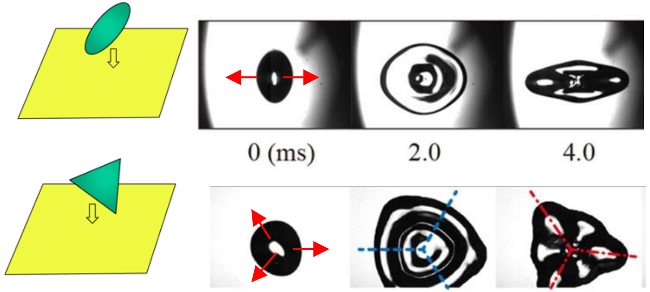

strongly-coupled cold atomic gas

$$L_{mfp} = 1/\rho\sigma$$

Science 298, 2179 (2002)

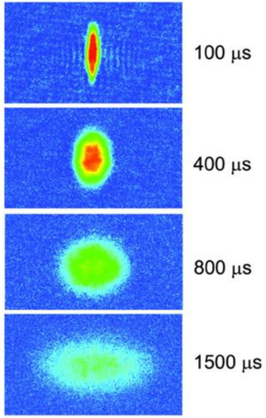

Coulomb Explosion Imaging in Chemistry

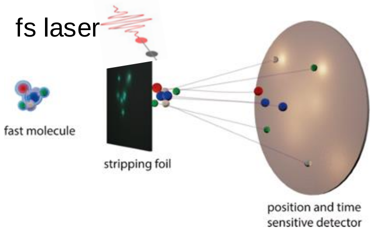

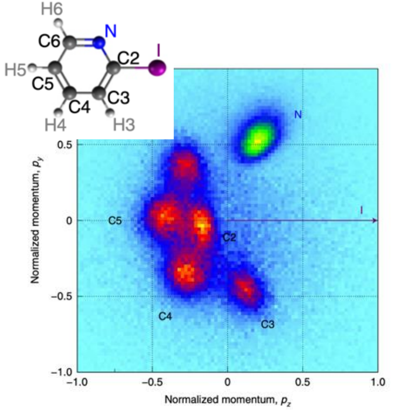

Instantaneous stripping of electrons and let atoms explode under mutual coulomb repulsion

Imaging by smashing: some examples

Smashing a deformed droplet on surface

$$F = \nabla P$$

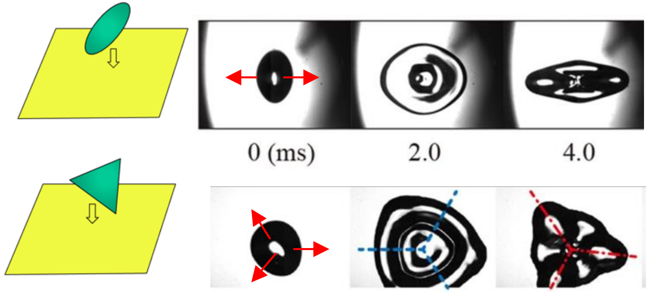

strongly-coupled cold atomic gas

$$L_{mfp} = 1/\rho\sigma$$

Science 298, 2179 (2002)

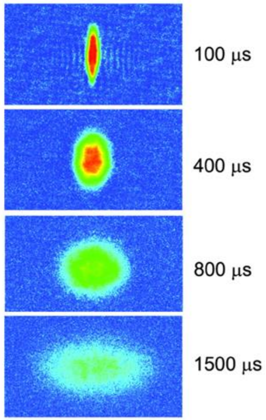

Coulomb Explosion Imaging in Chemistry

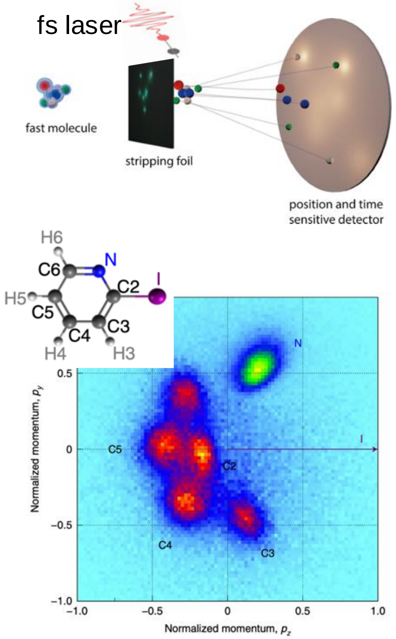

EOS, viscosity…

$$T_{\mu\nu}(\tau = 0) \qquad \partial_\mu T^{\mu\nu} = 0 \qquad T_{\mu\nu}(\tau = \infty)$$

snapshot → evolution → measurement

Image inferred after destruction

Instantaneous stripping of electrons and let atoms explode under mutual coulomb repulsion

Imaging by smashing: high-energy collisions

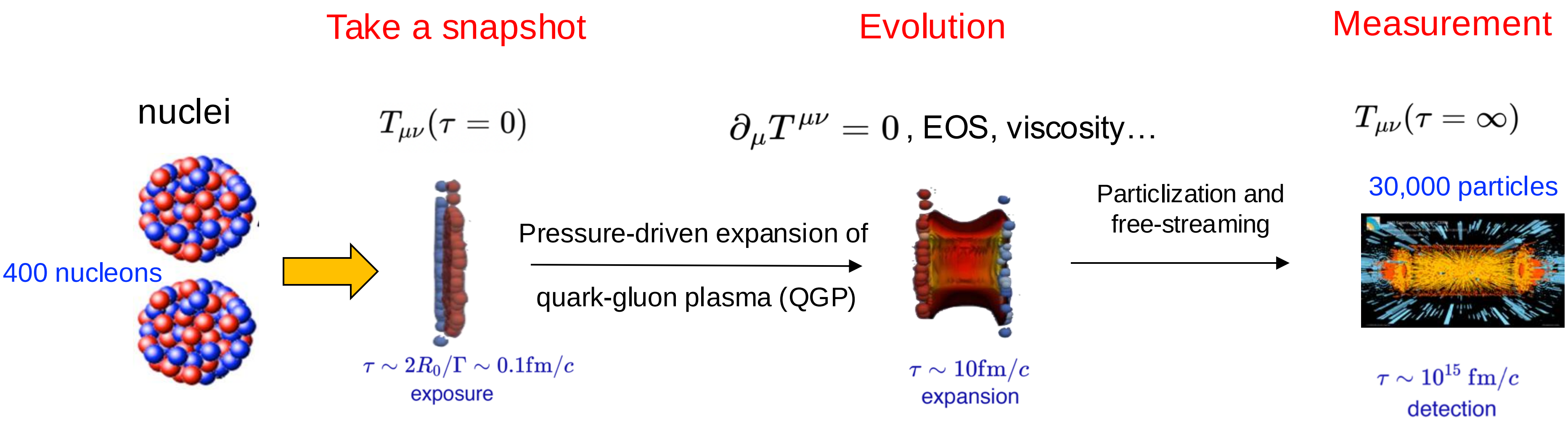

Large entropy production enable a semi-classical description

- Initial condition is a fast snapshot of nuclear structure
- Transformed to the final state via hydrodynamic expansion (EFT)
- Reverse-engineer to get snapshot, aided by large information output

Ability to image ←→ QGP dynamics and properties

Imaging by smashing: high-energy collisions

Take a snapshot

nuclei

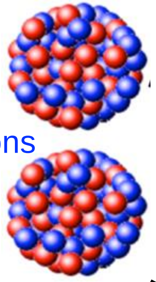

400 nucleons

$T_{\mu\nu}(\tau = 0)$

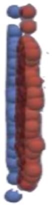

$\tau \sim 2R_0/\Gamma \sim 0.1\text{fm}/c$

exposure

$\int dz[\rho_1(x,y,z) + \rho_2(x+b,y,z)] \sim \rho_\perp(x,y)$

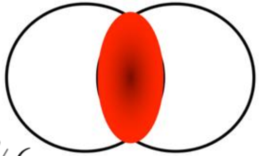

$R_\perp^2 \propto \langle r_\perp^2 \rangle$, $\mathcal{E}_n \propto \langle r_\perp^n e^{in\phi} \rangle$

size & shape

Evolution

$\partial_\mu T^{\mu\nu} = 0$, EOS, viscosity…

Pressure-driven expansion of quark-gluon plasma (QGP)

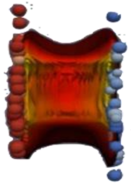

$\tau \sim 10\text{fm}/c$

expansion

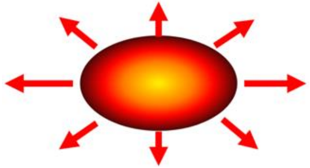

$$\frac{d^2N}{d\phi dp_T} = N(p_T)\left(\sum_n V_n\, e^{-in\phi}\right)$$

observables

Measurement

Particlization and free-streaming

$T_{\mu\nu}(\tau = \infty)$

30,000 particles

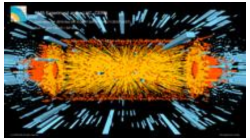

$\tau \sim 10^{15}$ fm$/c$

detection

Event-by-event linear responses:

$$V_n \propto \mathcal{E}_n$$

$$\frac{\delta[p_T]}{[p_T]} \propto -\frac{\delta R_\perp}{R_\perp}$$

Preserving the snapshot to the final state

Shape-flow transmutation via pressure-gradient force:

$$F = -\nabla P(\epsilon)$$

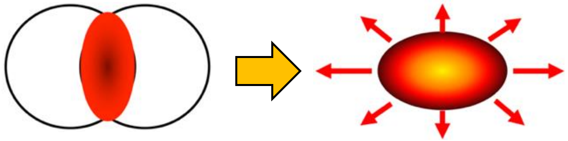

$$\frac{d^2N}{d\phi dp_T} = N(p_T)\left(\sum_n V_n\, e^{-in\phi}\right)$$

$$\frac{\delta[p_T]}{[p_T]} \propto -\frac{\delta R_\perp}{R_\perp}$$

$$V_n \propto \mathcal{E}_n$$

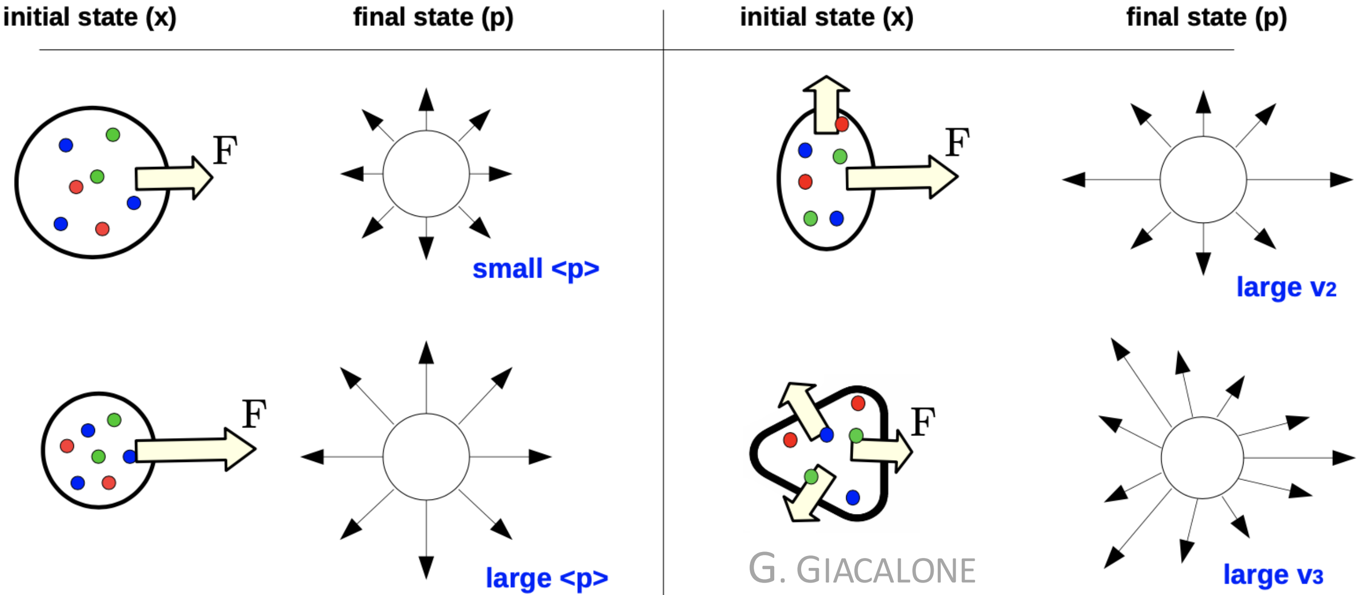

G. GIACALONE

Preserving the snapshot to the final state

Several real event display at LHC $T_{\mu\nu}(\tau=\infty)$

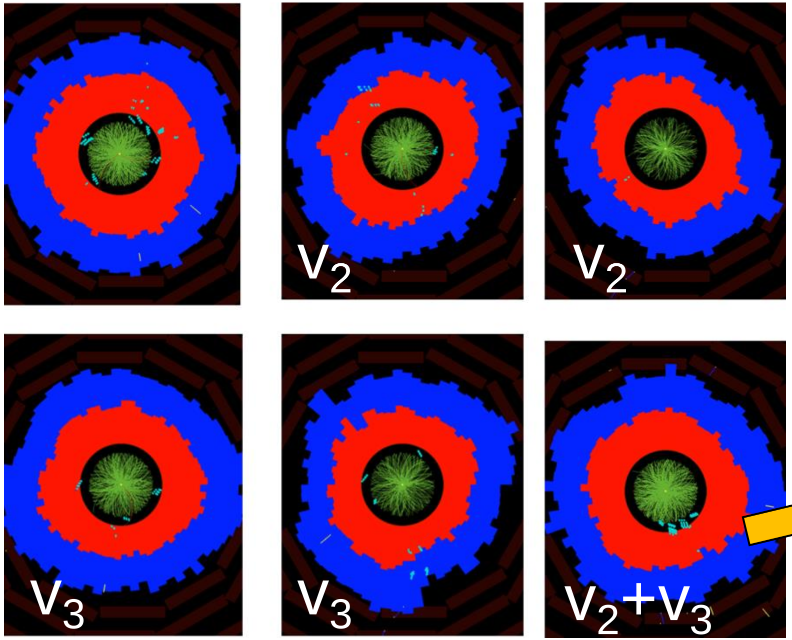

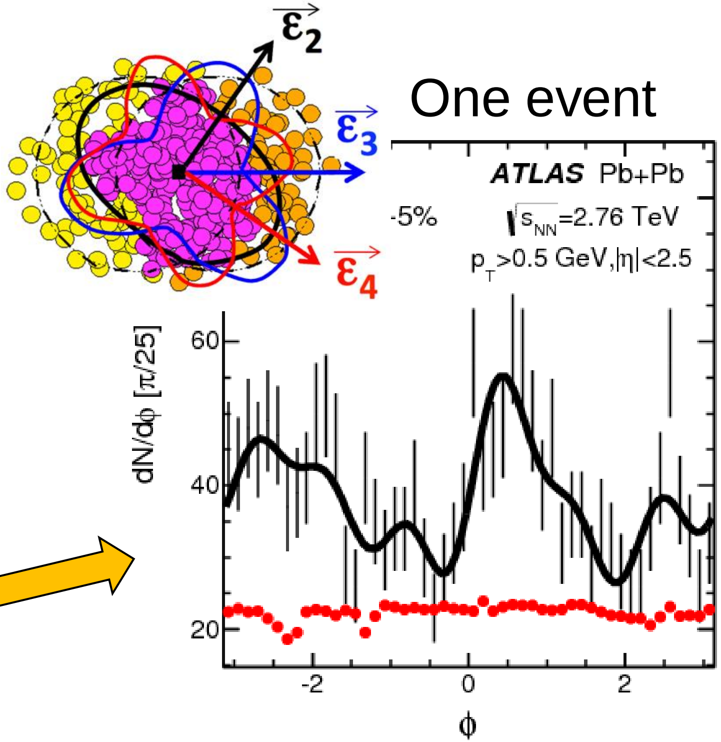

higher-order harmonics seen at single event level

Observables for event-by-event fluctuations

- Measure moments of p($1/R$, ε_2, ε_3…) via p([p_T], v_2, v_3…)…
  - Mean $\langle d_\perp \rangle$ ⟺ $\langle p_\mathrm{T} \rangle$
  - Variance: $\langle \varepsilon_n^2 \rangle$, $\left\langle (\delta d_\perp / d_\perp)^2 \right\rangle$ ⟺ $\langle v_n^2 \rangle$, $\left\langle (\delta p_\mathrm{T} / p_\mathrm{T})^2 \right\rangle$
  - Skewness $\langle \varepsilon_n^2 \delta d_\perp / d_\perp \rangle$, $\left\langle (\delta d_\perp / d_\perp)^3 \right\rangle$ ⟺ $\langle v_n^2 \delta p_\mathrm{T} / p_\mathrm{T} \rangle$, $\left\langle (\delta p_\mathrm{T} / p_\mathrm{T})^3 \right\rangle$
  - Kurtosis $\langle \varepsilon_n^4 \rangle - 2\langle \varepsilon_n^2 \rangle^2$, $\left\langle (\delta d_\perp / d_\perp)^4 \right\rangle - 3\left\langle (\delta d_\perp / d_\perp)^2 \right\rangle^2$ ⟺ $\langle v_n^4 \rangle - 2\langle v_n^2 \rangle^2$, $\left\langle (\delta p_\mathrm{T} / p_\mathrm{T})^4 \right\rangle - 3\left\langle (\delta p_\mathrm{T} / p_\mathrm{T})^2 \right\rangle^2$

  …

$$\mathcal{E}_n \equiv \varepsilon_n e^{ni\Phi_n} \propto \int_{\mathbf{r}} \mathbf{r}^n \rho(\mathbf{r}) \qquad d_\perp \propto - \int_{\mathbf{r}} |\mathbf{r}^2| \rho(\mathbf{r})$$

A plethora of measurements

- Single particle distribution   Flow vector: $\boldsymbol{V}_n = v_n e^{in\Psi_n}$

$$\frac{d^2N}{d\phi dp_{\mathrm{T}}} = N(p_T)\left[1 + 2\sum_n v_{\mathrm{n}}(p_T)\cos n(\phi - \Psi_n(p_T))\right]$$
$$= N(p_T)\left[\sum_{n=-\infty}^{\infty} V_{\mathrm{n}}(p_T)e^{in\phi}\right]$$

Radial flow   Anisotropic flow

- Two-particle correlation function

$$\left\langle \frac{d^2N_1}{d\phi dp_{\mathrm{T}}}\frac{d^2N_2}{d\phi dp_{\mathrm{T}}} \right\rangle \quad Þ \quad \langle \boldsymbol{V}_n(p_{T1})\boldsymbol{V}_n^*(p_{T2})\rangle \quad n - n = 0$$

- Multi-particle correlation function

$$\left\langle [p_{\mathrm{T}}]^k \frac{d^2N_1}{d\phi dp_{\mathrm{T}}} \ldots \frac{d^2N_m}{d\phi dp_{\mathrm{T}}} \right\rangle \Rightarrow \langle [p_{\mathrm{T}}]^k \boldsymbol{V}_{n_1}\boldsymbol{V}_{n_2}\ldots\boldsymbol{V}_{n_m}\rangle \qquad n_1 + n_2 + \ldots + n_m = 0$$

$$\downarrow$$

$$p([p_{\mathrm{T}}], \boldsymbol{V}_2, \boldsymbol{V}_3\ldots) = \frac{1}{N_{\mathrm{evts}}}\frac{dN_{\mathrm{evts}}}{d[p_{\mathrm{T}}]d\boldsymbol{V}_2 d\boldsymbol{V}_3\ldots}$$

EbyE fluctuations of size and shape

E-by-E flow amplitude distribution $p(v_n)$

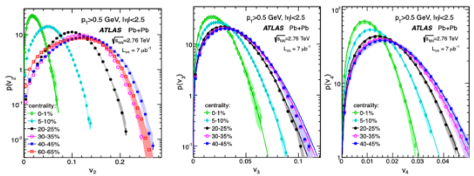

Higher-harmonics v_2-v_6

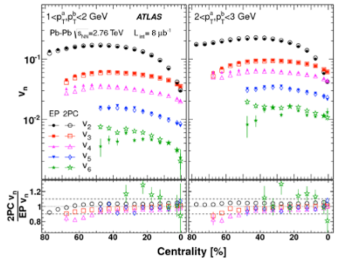

Event-plane correlation $p(\Psi_n,\Psi_m,\Psi_k)$

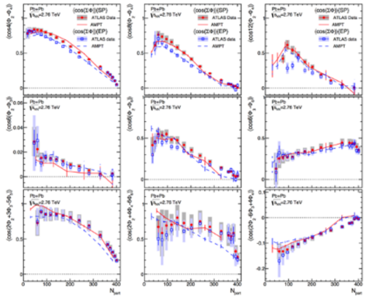

v_n-p_T correlation $p(v_n, p_T)$

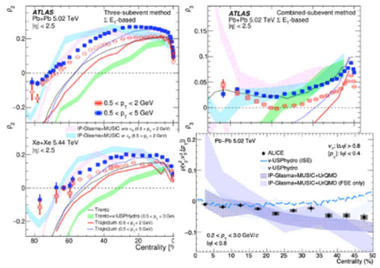

v_n amplitude correlation $p(v_n,v_m)$

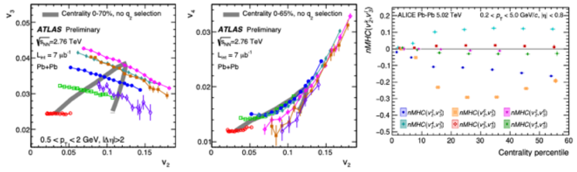

p_T fluctuations $p(p_T)$

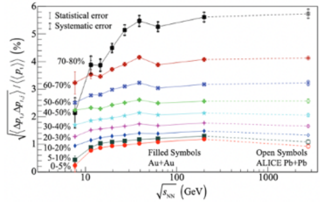

Seems we can infer the initial condition of QGP which carries imprints of the colliding nuclei.

But what kinds of images do we expect to get?

Intro to atomic nuclei at low energy

Many-body quantum systems, govern by short-range strong nuclear force
Emergent properties in between discrete nucleon and bulk nuclear matter, like quantum dot.
Configuration is one that minimizes E, which is often deformed away from magic numbers

Cluster of nucleons

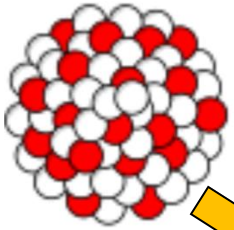

Magic numbers:
2 8 20 28 50 82 126

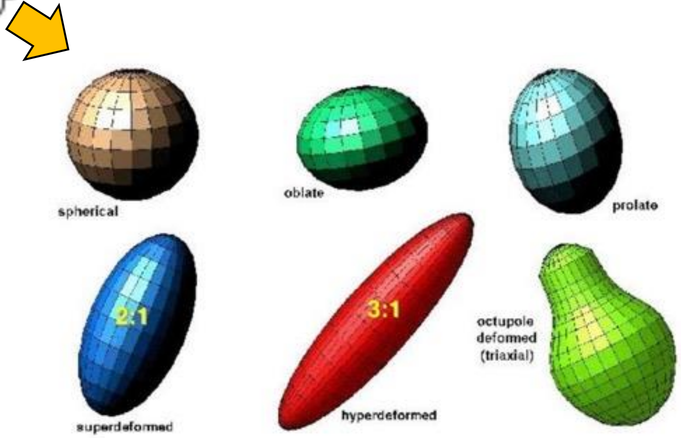

Cluster of atoms

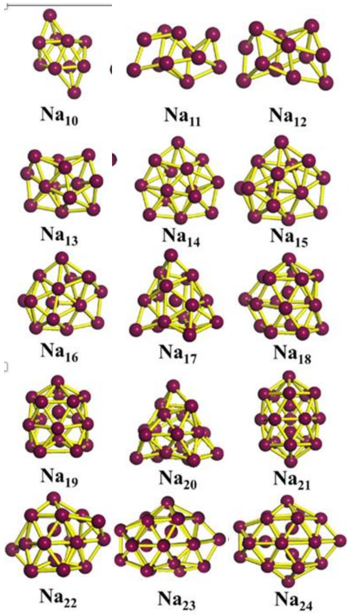

Na cluster

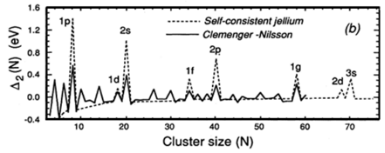

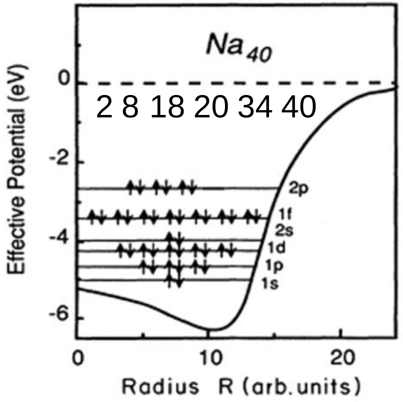

10.1021/acs.inorgchem.6b02340

Atomic nuclei and their shapes

Many-body quantum systems, govern by short-range strong nuclear force

Emergent properties in between bulk nuclear matter and discrete nucleon, like quantum doc.

Configuration is one that minimizes E, which is often deformed away from magic numbers

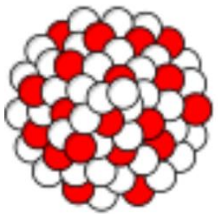

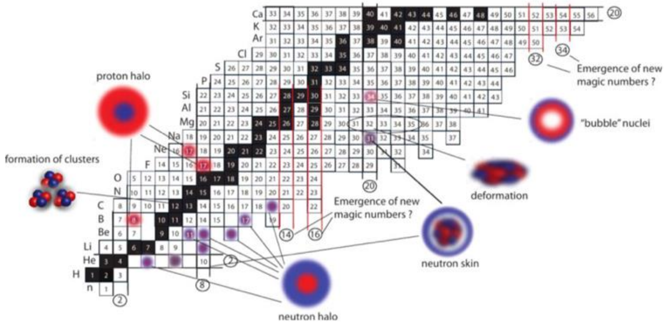

β_2-landscape

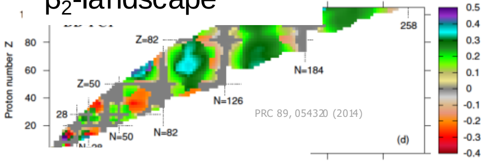

β_3-landscape

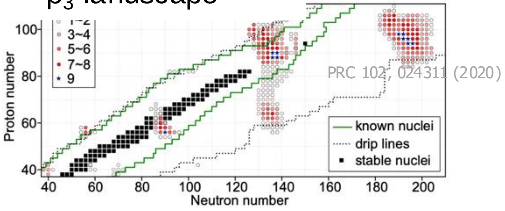

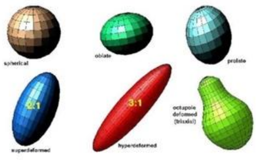

$$\rho(r,\theta,\phi) = \frac{\rho_0}{1+e^{(r-R(\theta,\phi))/a_0}}$$

$$R(\theta,\phi) = R_0(1+\beta_2[\cos\gamma Y_{2,0}(\theta,\phi)+\sin\gamma Y_{2,2}(\theta,\phi)] + \beta_3 Y_{3,0}(\theta,\phi) + \beta_4 Y_{4,0}(\theta,\phi))$$

$0 \le \gamma \le \pi/3$

Very rich landscape of shapes and other structures

Degrees-of-freedom and timescales

Heavy nuclei

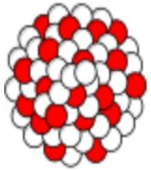

GR PR

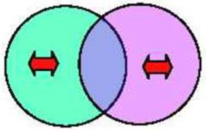

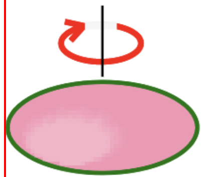

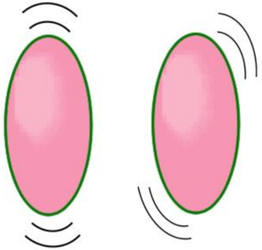

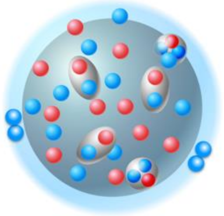

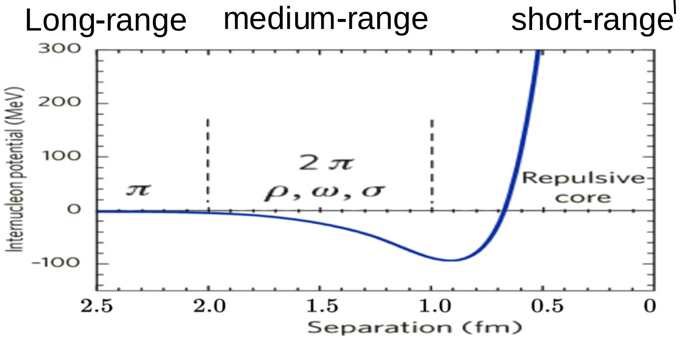

$$E = \frac{p^2}{2m}$$

	rotation	vibration	clustering	nucleon correlations
Energy scales: (MeV)	~0.1	~0.5-2	~a few	~1-50
Timescales: (fm/c)	10^4-10^3	~1000	~1000-100	~100 to a few

→ Quarks, gluons

Nuclear shapes at low energy: long exposure

Each DOF has zero-point fluctuations within certain timescale.

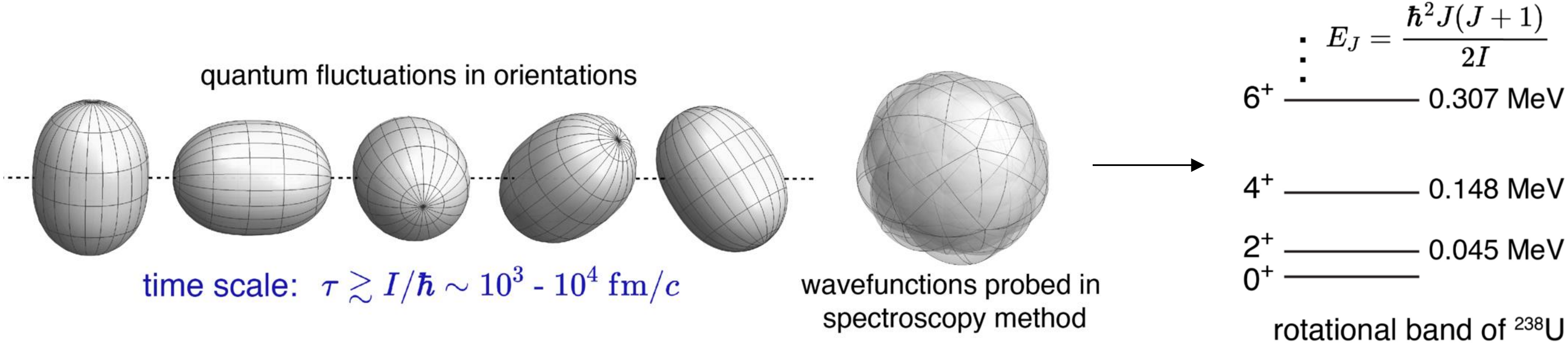

Spectroscopic methods probe a superposition of these fluctuations

Instantaneous shapes not directly seen→ intrinsic shape not observable at low E

Infer shape from model comparison to energy-transition-lifetime measurements.

Nuclear shape at high-energy: smashing experiment

To see event-by-event shape directly, one must have access to instantaneous many-body correlations $\Psi\left(\mathbf{r}_1, \mathbf{r}_2 \ldots\right)$

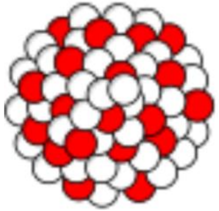

τ_{expo}

We will see all DOFs longer than this timescale: $\tau > \tau_{\text{expo}}$

Nucleons, hadrons, quark, gluons, gluon saturations

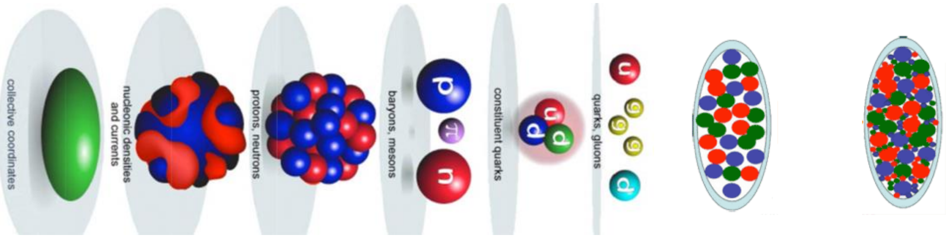

Concept of shape is collision energy dependent

$\epsilon_2 = 0$ $\qquad$ $\epsilon_2 \sim \frac{1}{\sqrt{A}}$

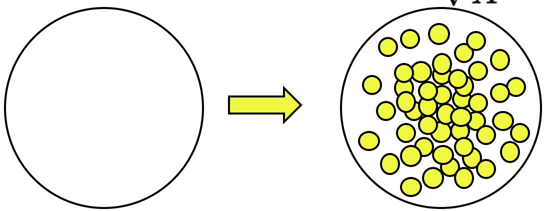

Spherical Woods-saxon $\qquad$ Sampled with A nucleons

$$\boldsymbol{\epsilon}_2 = \underbrace{\boldsymbol{\epsilon}_0}_{} + \underbrace{\boldsymbol{p}(\Omega)\beta_2}_{} + \mathcal{O}\left(\beta_2^2\right)$$

$\sqrt{s}$-dependent fluctuations induced shape

Global shape rotational vibrational

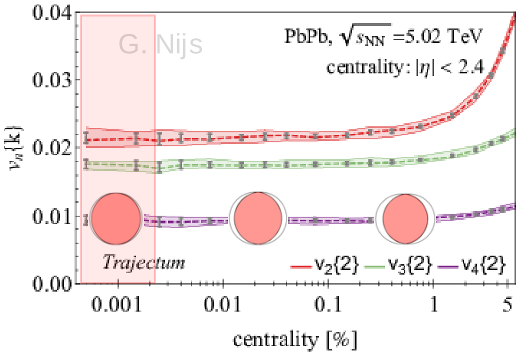

Smashing experiment and nuclear structure

Nuclear Structure

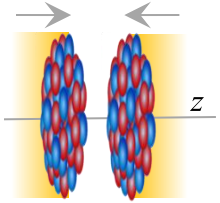

$$T_A(x,y) = \int \rho(x,y,z)dz$$

Shape and radial dis.

- $\beta_2 \rightarrow$ Quadrupole deformation
- $\beta_3 \rightarrow$ Octupole deformation
- $a_0 \rightarrow$ Surface diffuseness
- $R_0 \rightarrow$ Nuclear size

....

Nucleon width
Nucleon distance
substructure

Energy deposition

$$T \propto \left(\frac{T_A^p + T_B^p}{2}\right)^{q/p}$$

Initial condition

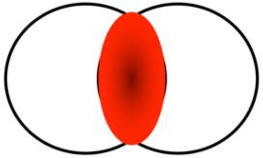

hydrodynamics

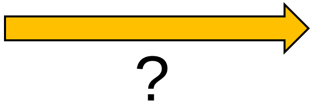

Size & shape

$$R_\perp^2 \propto \langle r_\perp^2 \rangle,\ \mathcal{E}_n \propto \langle r_\perp^n e^{in\phi} \rangle$$

Final state

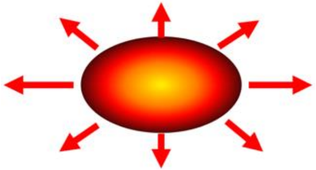

Observables

$$\frac{d^2N}{d\phi dp_T} = N(p_T)\left(\sum_n V_n\, e^{-in\phi}\right)$$

Precision of imaging method {
- space-time dynamics of QGP
- energy deposition mechanism

How to apply the method in practice?

Impact of deformation: head-on collisions

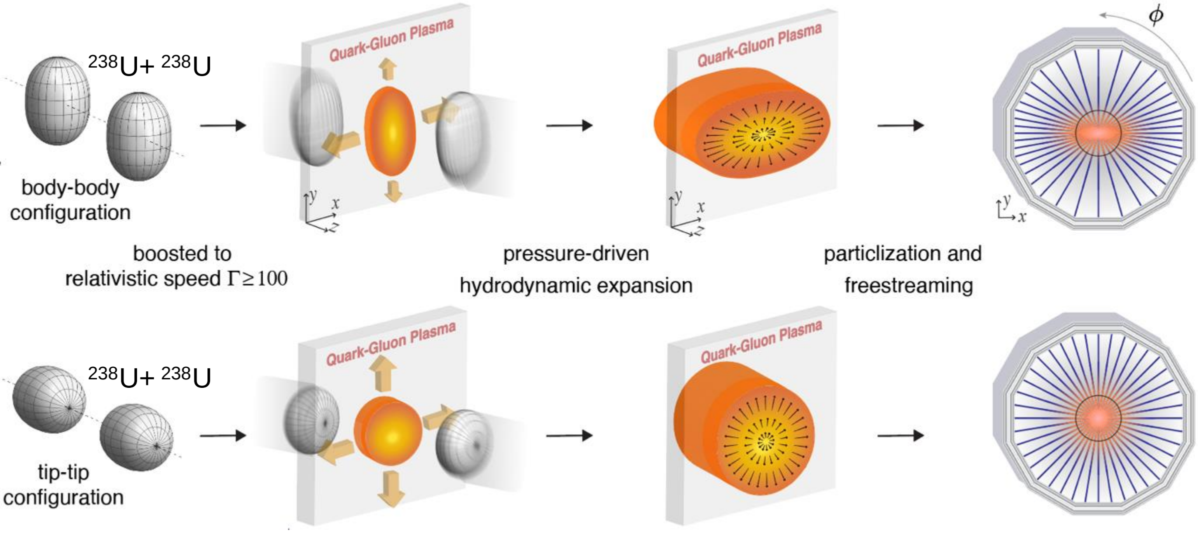

Collision geometry depends on the orientations: head-on collisions has two extremes body-body or tip-tip collisions

Body-body: large eccentricity large size

$v_2 \nearrow \quad p_T \searrow$

Tip-tip : small eccentricity small size

$v_2 \searrow \quad p_T \nearrow$

^{197}Au+ ^{197}Au | ^{238}U+ ^{238}U

$$\langle v_2^2 \rangle = a_1 + b_1 \beta_2^2 \ ,$$
$$\langle (\delta p_T)^2 \rangle = a_2 + b_2 \beta_2^2 \ ,$$
$$\langle v_2^2 \delta p_T \rangle = a_3 - b_3 \beta_2^3 \cos(3\gamma)$$

Compare to collision of near spherical ^{197}Au,

- Deformation enhances the fluctuations of v_2 and [p_T].
- and leads to anti-correlation between v_2 and [p_T].

Compare two systems to disentangle global deformation and quantum fluctuation!

low E　　　high E

Impact of deformation: head-on collisions

Seen directly by comparing ^{238}U+^{238}U with near-spherical ^{197}Au+^{197}Au

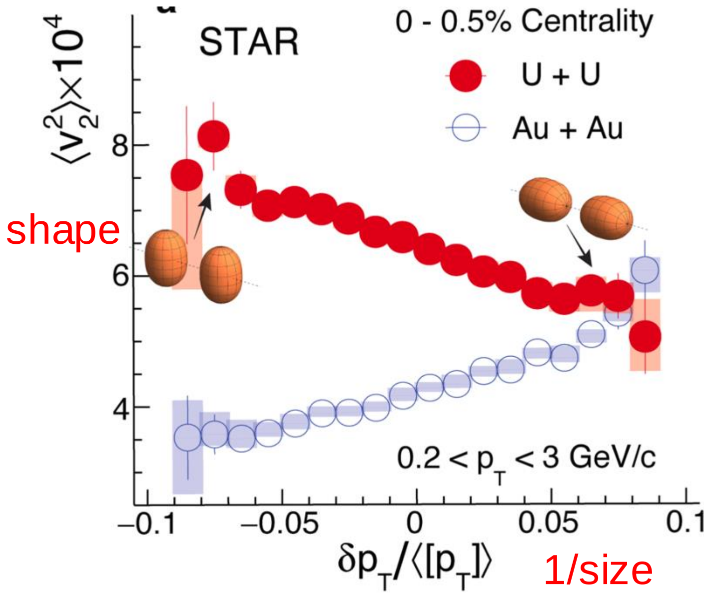

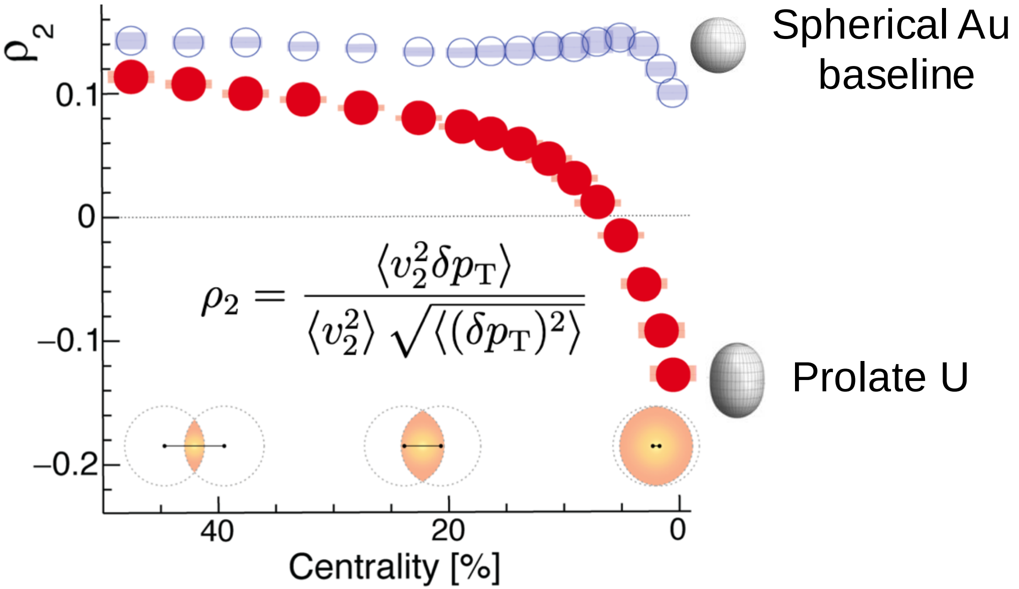

Near-spherical → flat ρ_2 vs centrality
Strongly prolate → decreasing of ρ_2 vs centrality

Ratio of observables $R_{\mathcal{O}} = \langle \mathcal{O} \rangle_{\mathrm{U+U}} / \langle \mathcal{O} \rangle_{\mathrm{Au+Au}}$

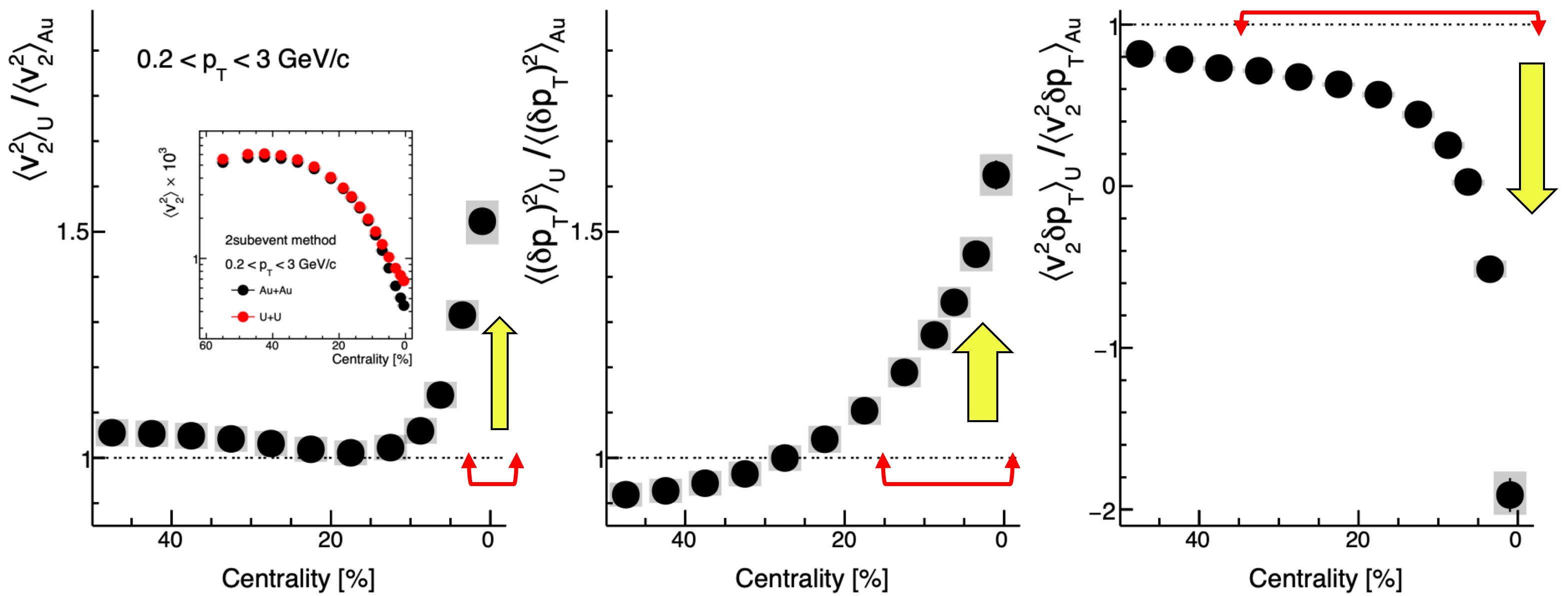

Ratios cancel final state effects and isolate the effects of initial state/nuclear structures!

U deformation dominates the ultra-central collisions (UCC)
→50%-70% impact on $\langle(\delta p_T)^2\rangle$ and $\langle v_2^2\rangle$, 300% for $\langle v_2^2 \delta p_T\rangle$

More smooth centrality dependence for $\langle(\delta p_T)^2\rangle$ than $\langle v_2^2\rangle$
→v_2 is dominated by v_2^{RP} (unaffected by deformation), having residual impact in UCC

Compared to hydrodynamic models

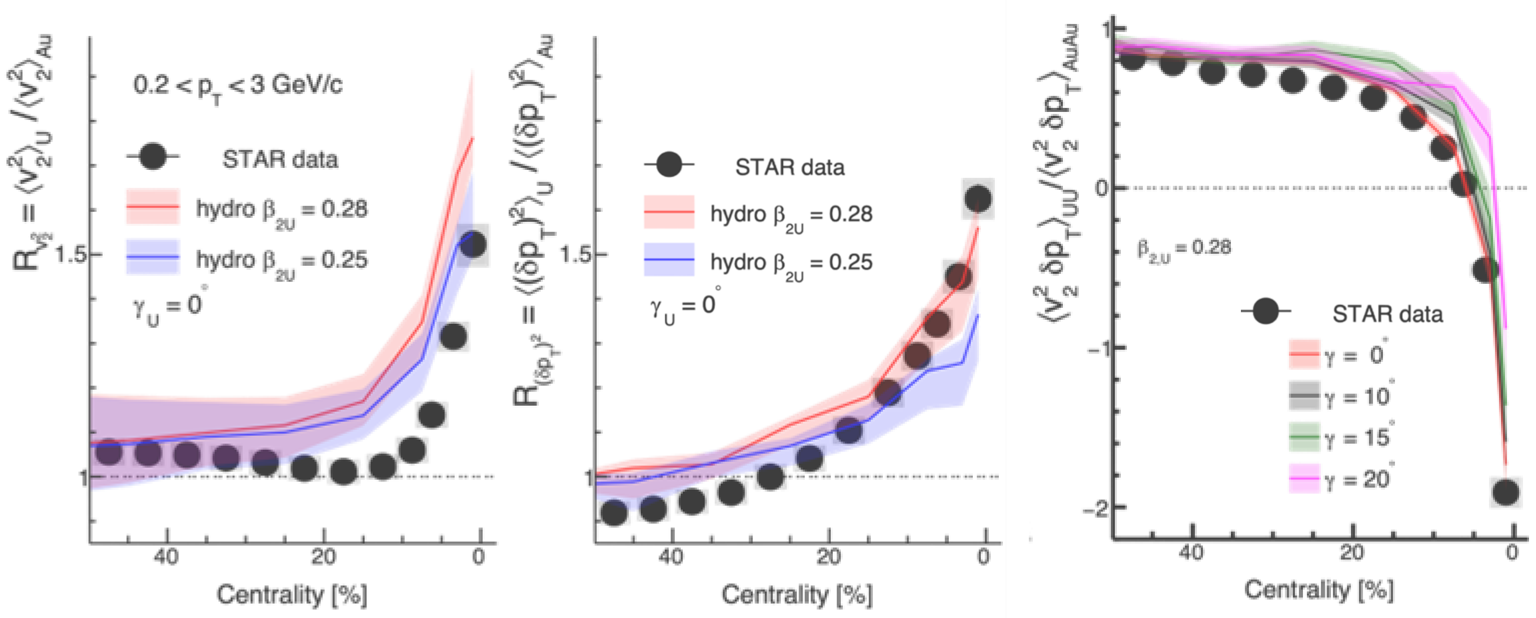

Compare with state-of-the-art ipglasma+music+UrQMD hydro model.

The $<(\delta p_T)^2>$ and $<v_2^2 \delta p_T>$ data seems prefers value closer to β_{2U} =0.28 and a small γ_U.

$<v_2^2>$ prefer a smaller β_{2U} value

Ratios cancel final state effects

- Vary the shear/bulk viscosity in Music hydro model
  - Flow signal change by more than factor of 2, yet the ratio unchanged.

$$v_2 \propto \varepsilon_2$$

$$\delta p_T \propto -\delta R$$

$$\frac{v_{2,\mathrm{U}}}{v_{2,\mathrm{Au}}} \approx \frac{\varepsilon_{2,\mathrm{U}}}{\varepsilon_{2,\mathrm{Au}}}$$

$$\frac{\langle(\delta p_T)^2\rangle_{\mathrm{U}}}{\langle(\delta p_T)^2\rangle_{\mathrm{Au}}} \approx \frac{\langle(\delta R)^2\rangle_{\mathrm{U}}}{\langle(\delta R)^2\rangle_{\mathrm{Au}}}$$

$$\frac{\langle v_2^2 \delta p_T\rangle_{\mathrm{U}}}{\langle v_2^2 \delta p_T\rangle_{\mathrm{Au}}} \approx \frac{\langle \varepsilon_2^2 \delta R\rangle_{\mathrm{U}}}{\langle \varepsilon_2^2 \delta R\rangle_{\mathrm{Au}}}$$

Robust probe of initial state!

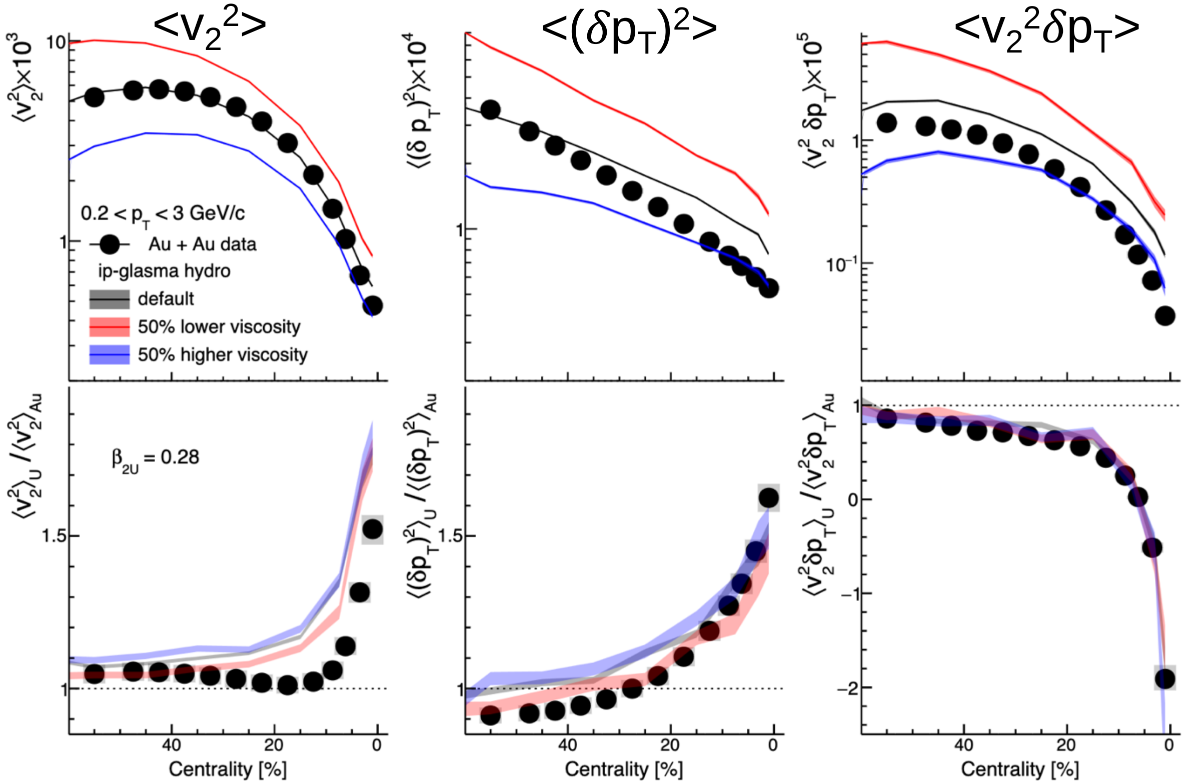

Sensitivity to other structure parameters

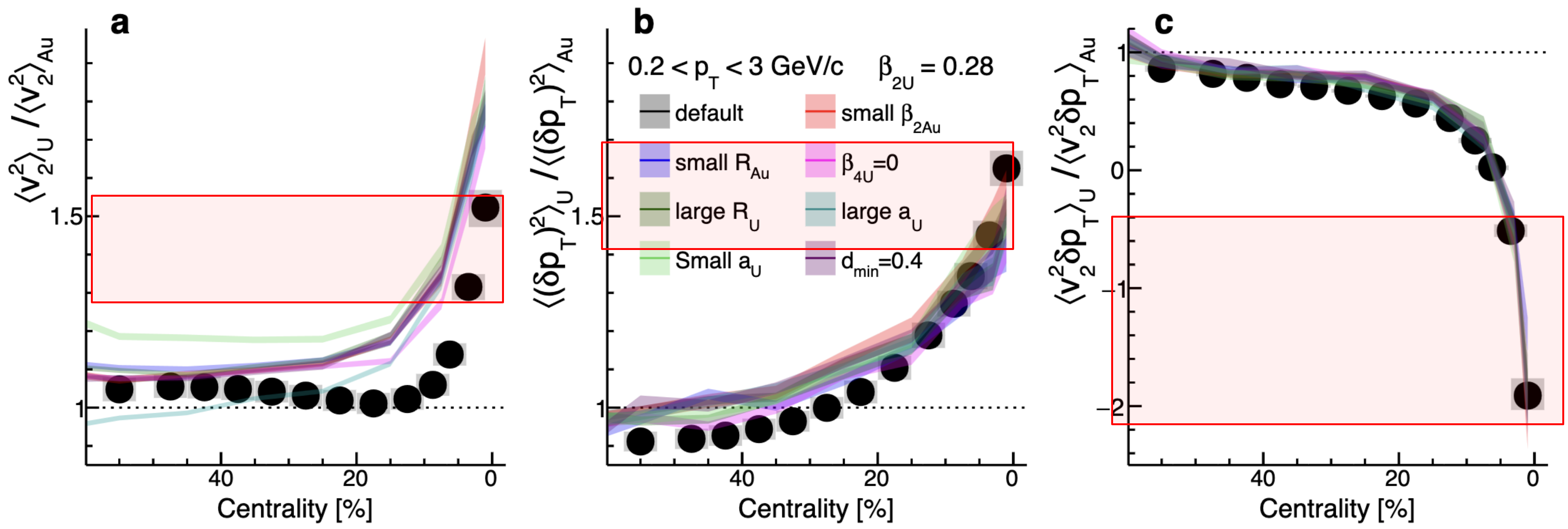

$$\rho(\vec{r}) = \frac{\rho_0}{1 + e^{(r - R_0(1+\sum_n \beta_n Y_n^0(\theta,\phi))/a_0}}$$

depend on other structure parameters:
R_0, a_0, higher-order deformation, nucleon separation

In ultra-central collisions, ratios are mainly controlled by β_{2U} and γ_U.

In non-central collisions, v_2 ratio is also sensitive to nuclear skin

Focus on 0-5% most central collisions to constrain the Uranium shape

Constraining the U238 shape

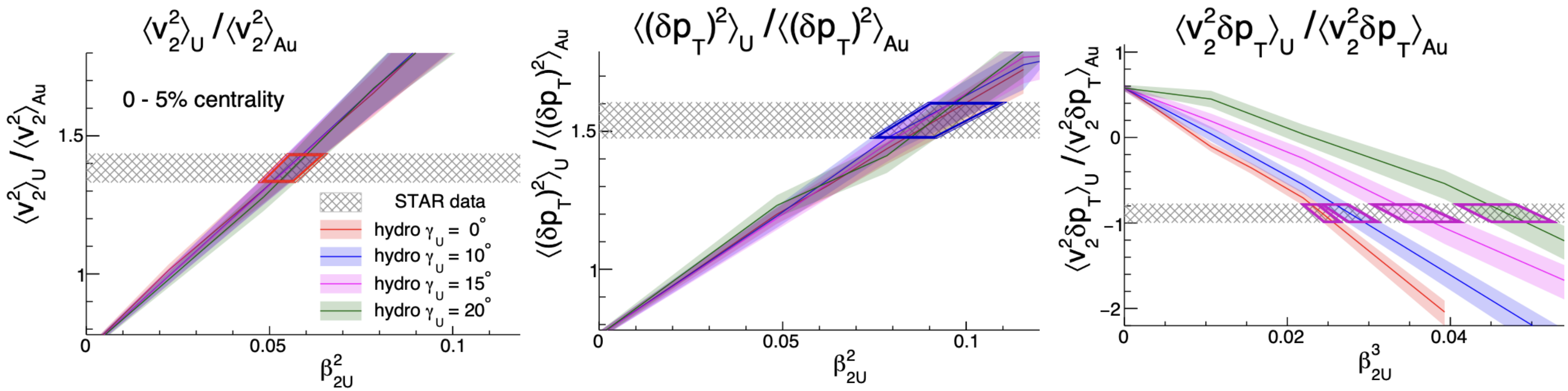

Confirming these relations, including strong sensitivity to triaxiality

focus on $\langle(\delta p_{\mathrm{T}})^2\rangle$, $\langle v_2^2 \delta p_{\mathrm{T}}\rangle$

$$\langle v_2^2\rangle = a_1 + b_1\beta_2^2 \,,$$
$$\langle(\delta p_{\mathrm{T}})^2\rangle = a_2 + b_2\beta_2^2 \,,$$
$$\langle v_2^2 \delta p_{\mathrm{T}}\rangle = a_3 - b_3\beta_2^3 \cos(3\gamma)$$

Results

High-energy estimate

$$\beta_{2U} = 0.286 \pm 0.025$$

$$\gamma_{\rm U} = 8.7^\circ \pm 4.5^\circ$$

Hydro-model uncertainties dominates

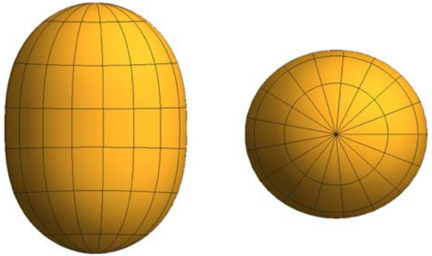

x-z

x-y

Low-energy estimate

$$\beta_{2U} = 0.287 \pm 0.007$$

$$\gamma_{\rm U} \sim 6^\circ - 8^\circ$$

With liquid model assumption

Global nuclear shape

$$\frac{\left\langle (\delta p_T)^2 \right\rangle_{\rm U}}{\left\langle (\delta p_T)^2 \right\rangle_{\rm Au}} \approx \frac{a_2 + b_2 \beta_{2U}^2}{a_2} = 1 + \frac{b_2}{a_2} \beta_{2U}^2$$

Spherical baseline, mainly from nucleon fluctuations. Described well by hydro model

Variations in energy deposition, saturation effects are subleading. Similar findings from B. Schenke. et.al

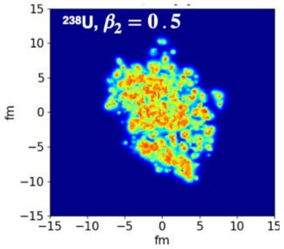

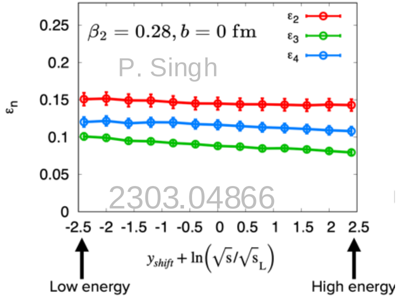

nature | Last updated Published on Nov 6 2024

Imaging shapes of atomic nuclei in high-energy nuclear collisions

Access & Citations

https://doi.org/10.1038/s41586-024-08097-2

45k	0	1
Article Accesses	Web of Science	CrossRef

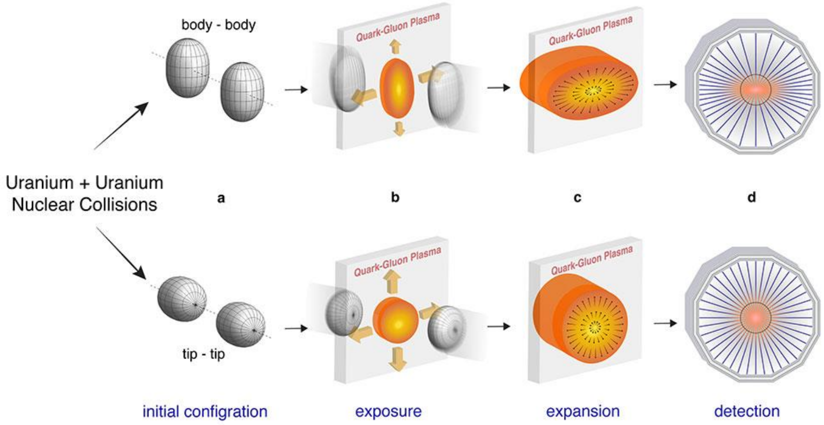

https://www.bnl.gov/newsroom/news.php?a=122119

nature

Explore content ⌄ About the journal ⌄ Publish with us ⌄ Subscribe

nature > news & views > article https://doi.org/10.1038/d41586-024-03466-3

NEWS AND VIEWS | 06 November 2024

Rare snapshots of a kiwi-shaped atomic nucleus

Smashing uranium-238 ions together proves to be a reliable way of imaging their nuclei. High-energy collision experiments reveal nuclear shapes that are strongly elongated and have no symmetry around their longest axis.

By Magda Zielińska & Paul E. Garrett

NEWS | 06 November 2024

Smashing atomic nuclei together reveals their elusive shapes

A method to take snapshots of exploding nuclei could hold clues about the fundamental properties of gold, uranium and other elements.

By Elizabeth Gibney https://www.nature.com/articles/d41586-024-03633-6

A general strategy for nuclear shape imaging

Flow observable = k $\otimes$ initial condition (structure)

QGP response,
a smooth function of N+Z

Structure of colliding nuclei,
non-monotonic function of N and Z

Compare two systems X and Y of same mass but different structure

$$R_{\mathcal{O}} \equiv \frac{\mathcal{O}_{\mathrm{X+X}}}{\mathcal{O}_{\mathrm{Y+Y}}} \approx 1 + c_1 \Delta\beta_2^2 + c_2 \Delta\beta_3^2 + c_3 \Delta R_0 + c_4 \Delta a$$

arXiv: 2111.15559

Deviation from unity depends only on their structural differences
c_1 - c_4 directly probes energy deposition mechanism in the initial condition!

Isobar $^{96}Ru+^{96}Ru$ and $^{96}Zr+^{96}Zr$ collisions at RHIC 200 GeV

^{96}Ru= 44 p + 52 n
^{96}Zr = 40 p + 56 n

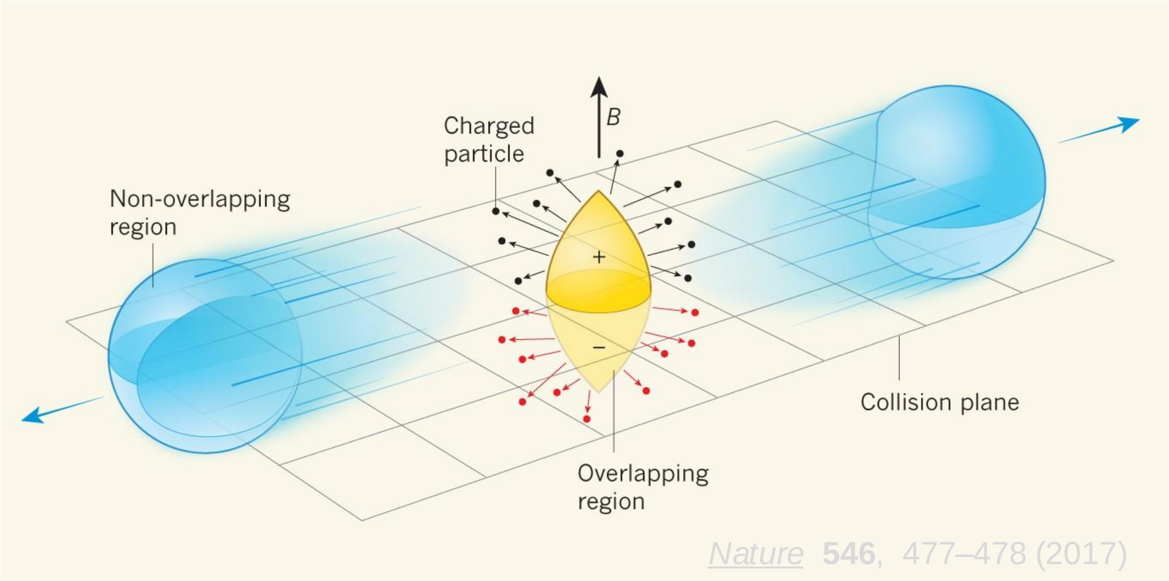

Originally designed to search for exotic magnetic effects

Isobar ^{96}Ru+^{96}Ru and ^{96}Zr+^{96}Zr collisions at RHIC 200 GeV

QM2022 poster, Chunjian Zhang

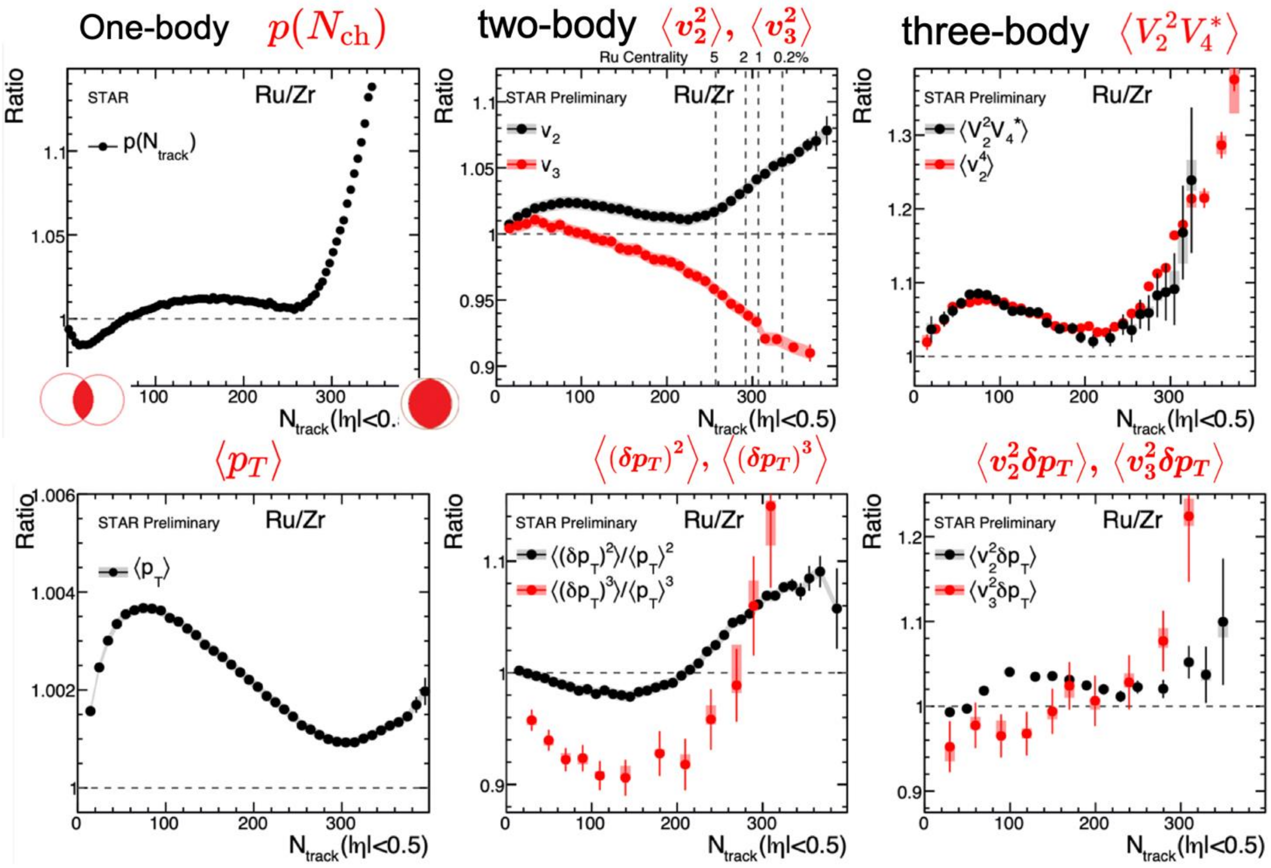

$$R_{\mathcal{O}} \equiv \frac{\mathcal{O}_{Ru}}{\mathcal{O}_{Zr}}$$

Structure influences everywhere

Opportunity for precision structure study

Nuclear structure via v_2-ratio and v_3-ratio

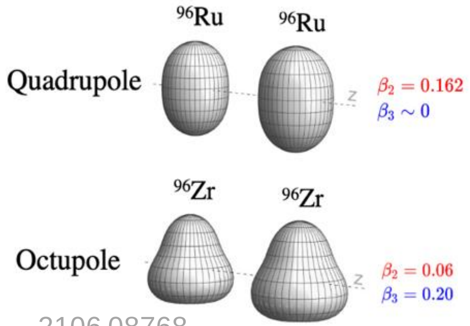

2106.08768

Species	β_2	β_3	a_0	R_0
Ru	0.162	0	0.46 fm	5.09 fm
Zr	0.06	0.20	0.52 fm	5.02 fm
difference	$\Delta\beta_2^2$	$\Delta\beta_3^2$	Δa_0	ΔR_0
	0.0226	-0.04	-0.06 fm	0.07 fm

$$R_{\mathcal{O}} \equiv \frac{\mathcal{O}_{\mathrm{Ru}}}{\mathcal{O}_{\mathrm{Zr}}} \approx 1 + c_1\Delta\beta_2^2 + c_2\Delta\beta_3^2 + c_3\Delta R_0 + c_4\Delta a$$

2109.00131

Simultaneously constrain four structure parameters

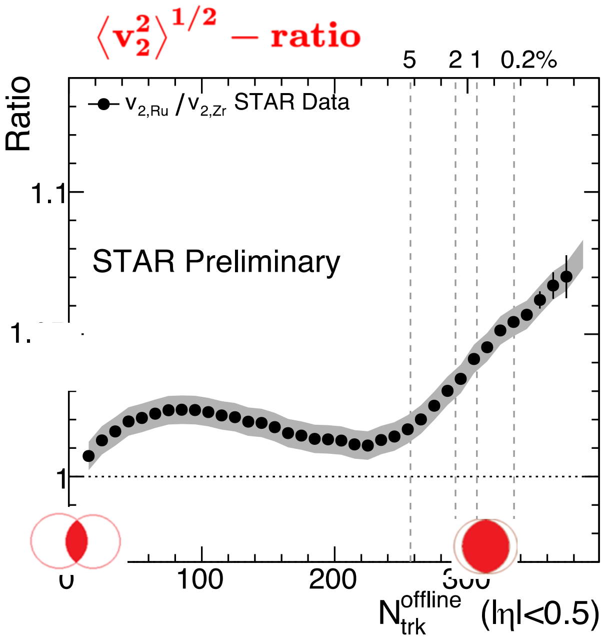

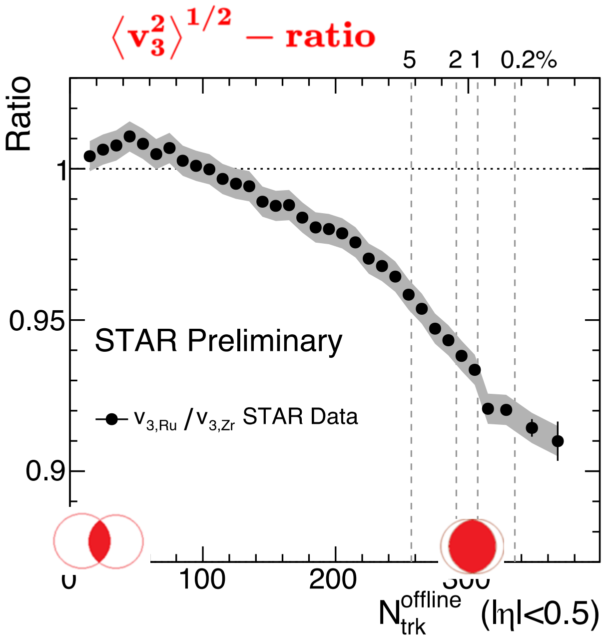

Nuclear structure via v_2-ratio and v_3-ratio

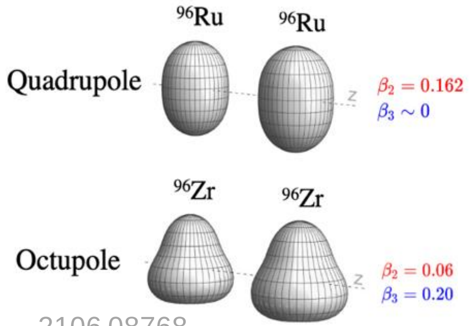

2106.08768

Species	β_2	β_3	a_0	R_0
Ru	0.162	0	0.46 fm	5.09 fm
Zr	0.06	0.20	0.52 fm	5.02 fm
difference	$\Delta\beta_2^2$	$\Delta\beta_3^2$	Δa_0	ΔR_0
	0.0226	-0.04	-0.06 fm	0.07 fm

- $\beta_{2Ru} \sim 0.16$ increase v_2, no influence on v_3 ratio
- $\beta_{3Zr} \sim 0.2$ decrease v_2 and v_3 ratio
- $\Delta a_0 = -0.06$ fm increase v_2 mid-central,
- Radius $\Delta R_0 = 0.07$ fm slightly affects v_2 and v_3 ratio.

Is ^{96}Zr octupole deformed?

$$R_{\mathcal{O}} \equiv \frac{\mathcal{O}_{\mathrm{Ru}}}{\mathcal{O}_{\mathrm{Zr}}} \approx 1 + c_1\Delta\beta_2^2 + c_2\Delta\beta_3^2 + c_3\Delta R_0 + c_4\Delta a$$

2109.00131

Simultaneously constrain four structure parameters

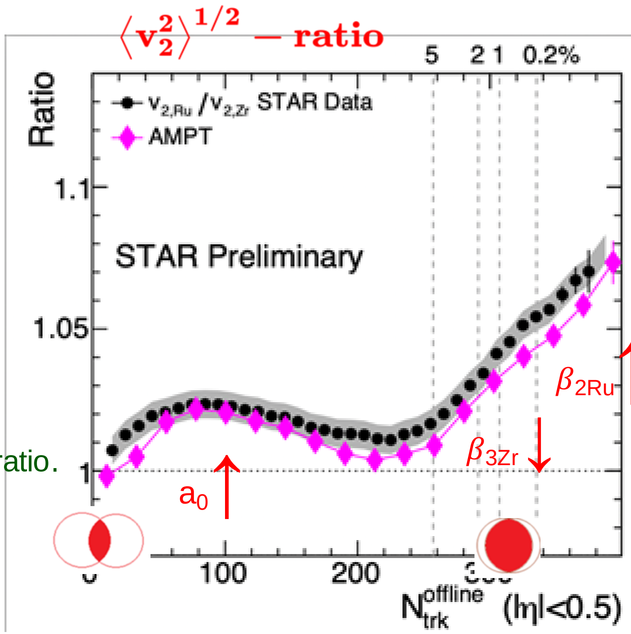

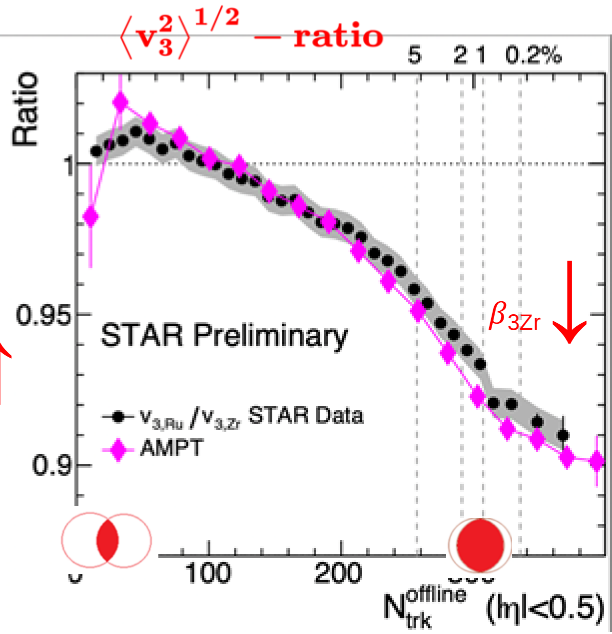

Currently available collision systems

RHIC $\sqrt{s}$=200GeV		LHC $\sqrt{s}$=5000 GeV
$^{197}Au+^{197}Au$ vs $^{238}U+^{238}U$ β_{2U} γ_U β_{3U} β_{4U}	**Establish methodology** • Large sensitivity	$^{129}Xe+^{129}Xe$ vs $^{208}Pb+^{208}Pb$ β_{2Xe} γ_{Xe} Neutron skin
$^{96}Ru+^{96}Ru$ vs $^{96}Zr+^{96}Zr$ β_{2Ru} β_{3Zr} large skin	**Establish precision** • 0.2% measurement error vs 5-15% signal • High-order observables	
d+^{197}Au vs $^{16}O+^{16}O$	**Structure of light nuclei** • Cluster, subnucleon structure. • Benchmark ab-initio models	$^{16}O+^{16}O$ vs $^{20}Ne+^{20}Ne$?
p+p, p+^{27}Al, p+^{197}Au, $^{3}He+^{197}Au$, $^{63}Cu+^{63}Cu$, $^{63}Cu+^{197}Au$	What can we learn from these?	p+p, p+^{16}O, p+^{208}Pb

What other species to consider & what questions do they answer?

Future opportunities

High-energy: fast snapshot of nucleon distribution for any collision species.
Low-energy: complexity & interpretation depends on location in nuclide chart

constrain initial condition via
nuclei with known structure

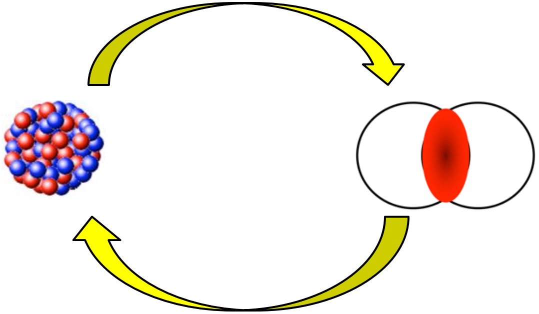

Constrain the structure for nuclei of
interest with known initial condition

Better constrains on properties of QGP

Current extraction of QGP properties
are limited by the initial condition

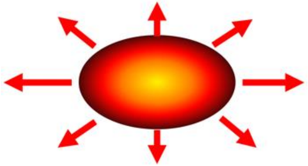

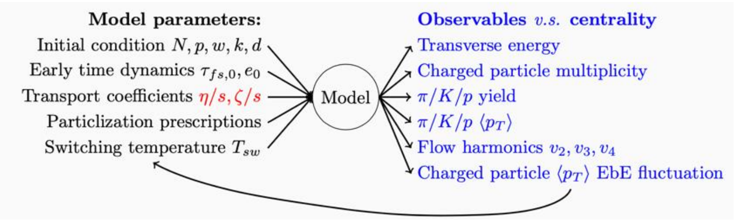

effective for discerning shape differences between isobar-like species

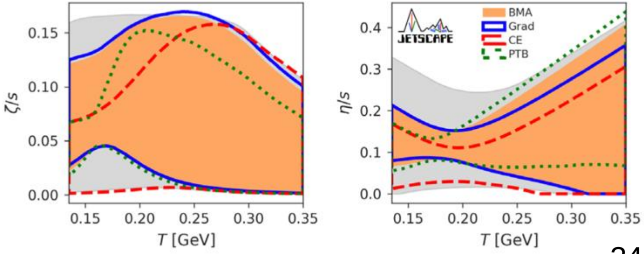

With the imaging-by-smashing tool polished, many exciting applications lie ahead

Odd N or Z nuclei

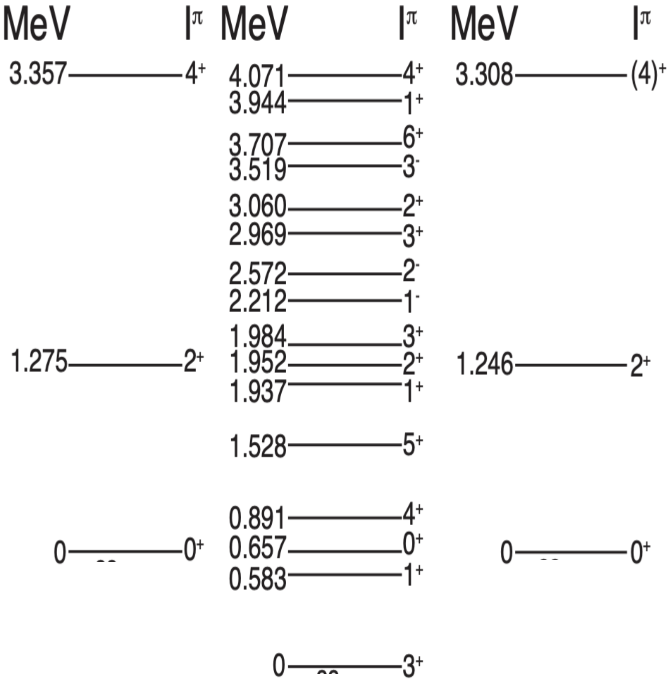

$^{22}_{10}Ne$ $^{22}_{11}Na$ $^{22}_{12}Mg$

nuclear shape is often presumed to be similar to adjacent even-even nuclei.

their spectroscopic data are more complex due to the coupling of the single unpaired nucleon with the nuclear core.

by comparing the flow observables of odd-mass nuclei to selected even-even neighbors with established shapes, the high-energy approach avoids this complication.

Higher-order deformations β_3 and β_4

Ratio of v_n in UCC region are mainly sensitive to β_n

$$\langle v_2^2 \rangle \approx a_2 + b_{2,2}\beta_2^2 + b_{2,3}\beta_3^2$$
$$\langle v_3^2 \rangle \approx a_3 + b_{3,3}\beta_3^2 + b_{3,4}\beta_4^2$$
$$\langle v_4^2 \rangle \approx a_4 + b_{4,4}\beta_4^2$$

Uranium 238

β_2	β_3	β_4
0.286[12]	0.078[13]	0.07 – 0.09[14, 15]

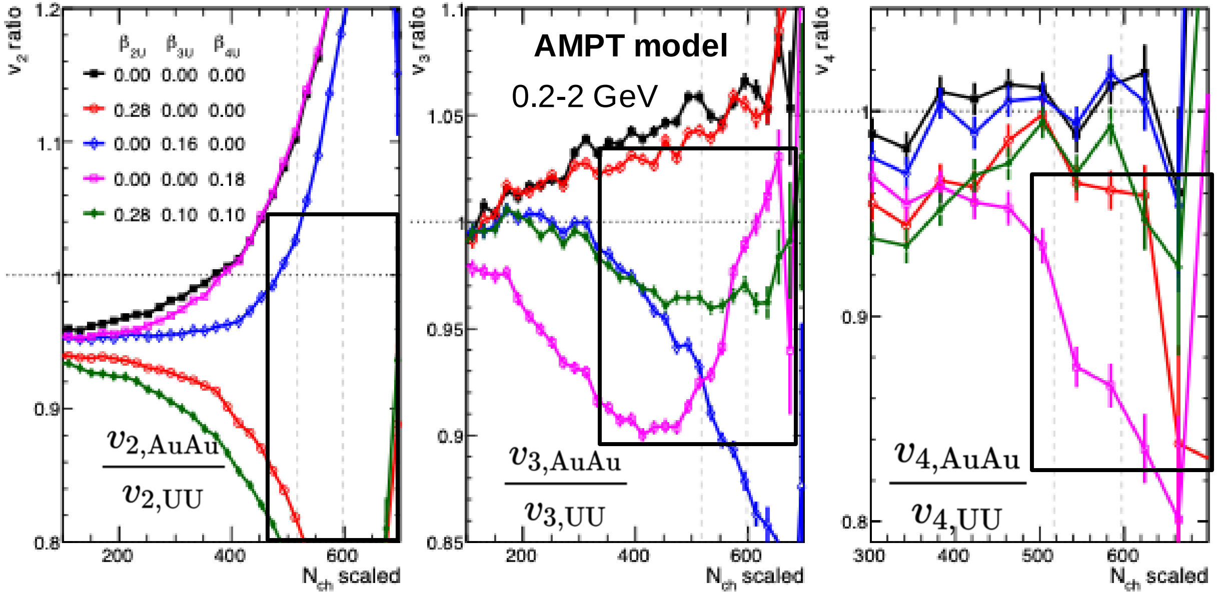

β_{4U} constrained using v_4 ratio in central region

Order of v_3 reversed by considering non-zero β_{3U} β_{4U}

v_2 ratio is mostly affected by β_{2U}, but also β_{3U}

Shape fluctuation and coexistence

Same nuclei can have several low-lying states with different intrinsic shapes

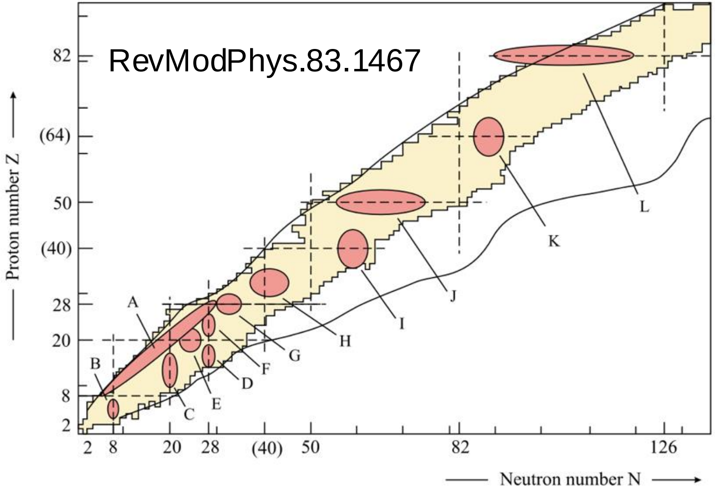

High-energy collisions are sensitive only to ground state shape, avoid shape variations during transitions

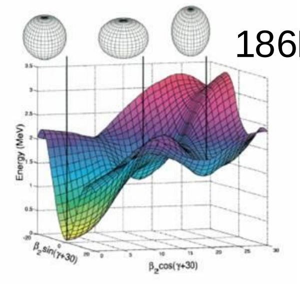

Nature **405**,430 (2000)

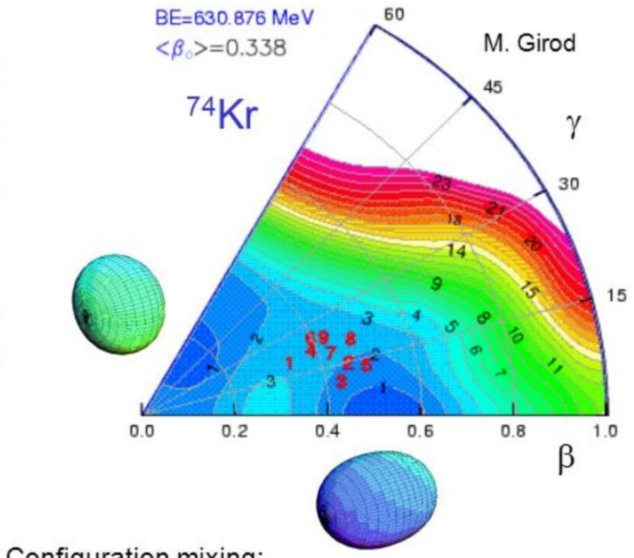

Configuration mixing:

$$|0_1^+\rangle = +\cos\eta\,|0_{\rm pro}^+\rangle + \sin\eta\,|0_{\rm obl}^+\rangle$$

$$|0_2^+\rangle = -\sin\eta\,|0_{\rm pro}^+\rangle + \cos\eta\,|0_{\rm obl}^+\rangle$$

electric monopole (E0) transition

$$\langle 0_2^+\|\mathbf{M}(E0)\|0_1^+\rangle \propto \sin\eta\cos\eta\,(\beta_{\rm pro}^2 - \beta_{\rm obl}^2)$$

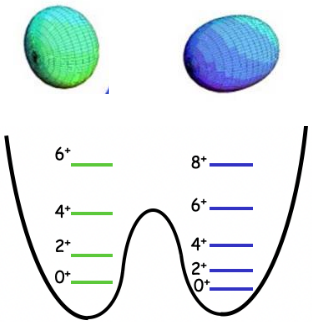

HI collision to probe shape entanglement!

Shape fluctuations via high-order correlations.

$$\left\langle (\delta p_{\mathrm{T}})^2 \right\rangle = a_2 + b_2 \beta_2^2 \,,$$
$$\left\langle v_2^2 \delta p_{\mathrm{T}} \right\rangle = a_3 - b_3 \beta_2^3 \cos(3\gamma)$$

$$\langle \beta_2^2 \rangle = \bar{\beta}_2^2 + \sigma_{\beta_2}^2 \qquad \langle \cos(3\gamma)^2 \rangle = \overline{\cos(3\gamma)}^2 + \sigma_{\cos(3\gamma)^2}$$

two- or three-particle correlations can't distinguish between static β_2,γ from their fluctuations.

Equal mix of prolate and oblate looks like triaxial

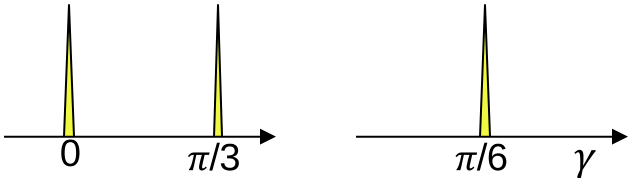

$$\langle \cos(3\gamma) \rangle = 0$$

STAR U238 measurement doesn't distinguish between static γ or γ fluctuations

Shape fluctuations via high-order correlations.

$$\left\langle (\delta p_{\mathrm{T}})^2 \right\rangle = a_2 + b_2 \beta_2^2 \,,$$
$$\left\langle v_2^2 \delta p_{\mathrm{T}} \right\rangle = a_3 - b_3 \beta_2^3 \cos(3\gamma)$$

$$\langle \beta_2^2 \rangle = \bar{\beta}_2^2 + \sigma_{\beta_2}^2 \qquad \langle \cos(3\gamma)^2 \rangle = \overline{\cos(3\gamma)}^2 + \sigma_{\cos(3\gamma)^2}$$

two- or three-particle correlations can't distinguish between static β_2,γ from their fluctuations.

Equal mix of prolate and oblate looks like triaxial

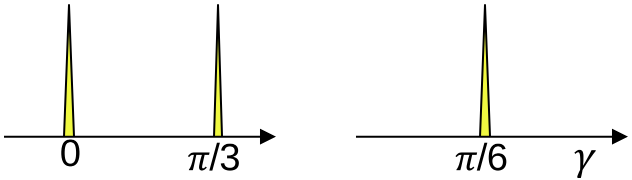

$$\langle \cos(3\gamma) \rangle = 0$$

STAR U238 measurement doesn't distinguish between static γ or γ fluctuations

Need higher-order correlators to disentangle mean and variance of β_2 and γ

$$v_2 \propto \varepsilon_2$$

$$\delta d_\perp / d_\perp \propto \delta[p_T]/[p_T]$$

Heavy ion observables:

arXiv:2301.03556

$$\frac{\langle \varepsilon_2^2 \rangle}{\frac{3}{4\pi}\langle \beta_2^2 \rangle} \Longleftrightarrow \frac{\langle \varepsilon_2^4 \rangle - 2\langle \varepsilon_2^2 \rangle^2}{-\frac{9}{112\pi^2}\left(7\langle \beta_2^2 \rangle^2 - 5\langle \beta_2^4 \rangle\right)}$$

$$\frac{\langle \varepsilon_2^2 (\delta d_\perp / d_\perp) \rangle}{-\frac{3\sqrt{5}}{112\pi^{3/2}}\langle \cos(3\gamma)\beta_2^3 \rangle} \Longleftrightarrow \frac{\left(\langle \varepsilon_2^6 \rangle - 9\langle \varepsilon_2^4 \rangle \langle \varepsilon_2^2 \rangle + 12\langle \varepsilon_2^2 \rangle^3\right)/4}{\frac{81}{256\pi^3}\left[\langle \beta_2^2 \rangle^3 - \frac{45}{14}\langle \beta_2^4 \rangle \langle \beta_2^2 \rangle - \frac{1175}{6006}\langle \beta_2^6 \rangle + \frac{25}{3003}\langle \cos(6\gamma)\beta_2^6 \rangle\right]}$$

$$2\langle \cos(6\gamma) \rangle = \langle \cos(3\gamma)^2 \rangle + 1$$

Neutrinoless double-beta decay

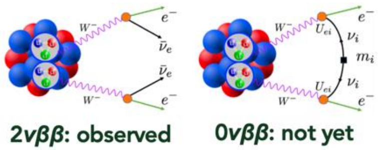

Phase space

Mass parameter

$$[T^{0\nu}_{1/2}]^{-1} = G_{0\nu}(Q,Z)|M_{0\nu}|^2\langle m_{\beta\beta}\rangle^2$$

Nuclear matrix element

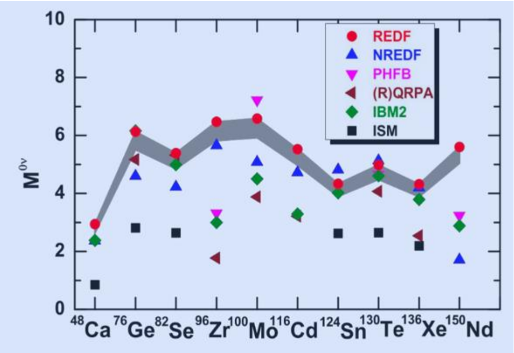

Need to model the overlap of nuclear wavefunction between **initial nuclei and its final isobar nuclei**.

Uncertainty in matrix element leads to x10 change in lifetime

Isobar collisions allow us to determine their shape differences, thus could help reduce the uncertainty of NME.

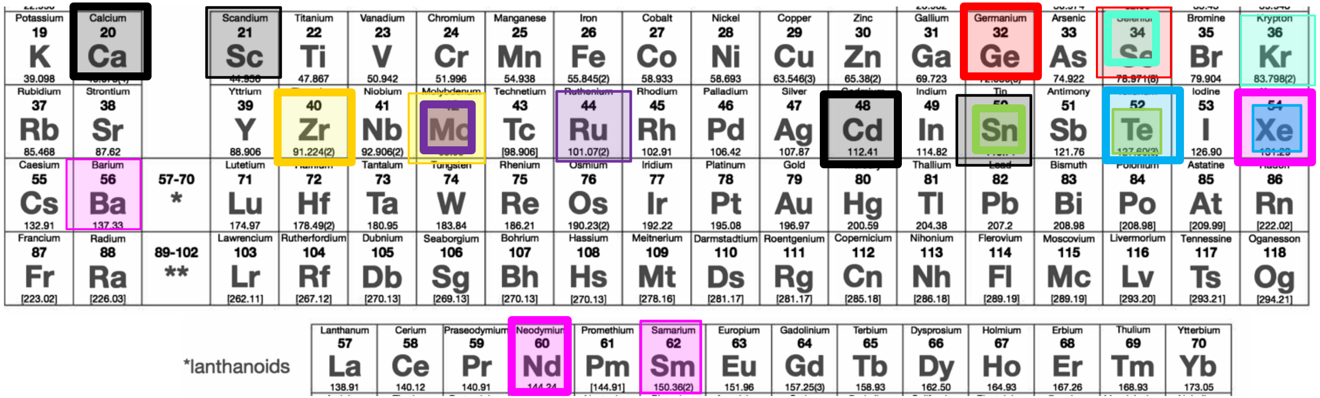

Imaging the radial structure: $\rho(\vec{r}) = \frac{\rho_0}{1+e^{(r-R_0(1+\sum_n \beta_n Y_n^0(\theta,\phi))/a_0}}$

- Radial parameters R_0, a_0 are properties of one-body distribution → **$\langle p_T \rangle$, $\langle N_{ch} \rangle$, v_2^{RP}~$v_2\{4\}$, σ_{tot},**

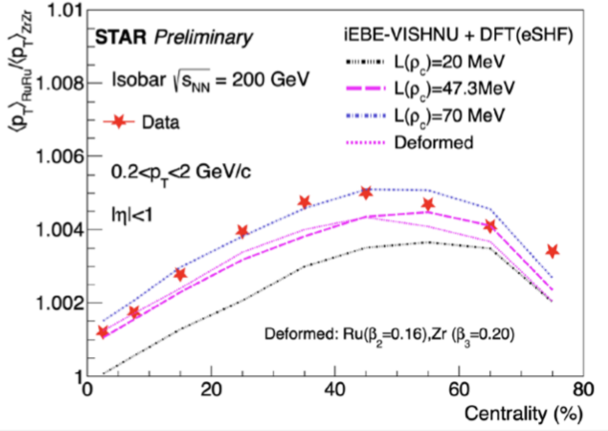

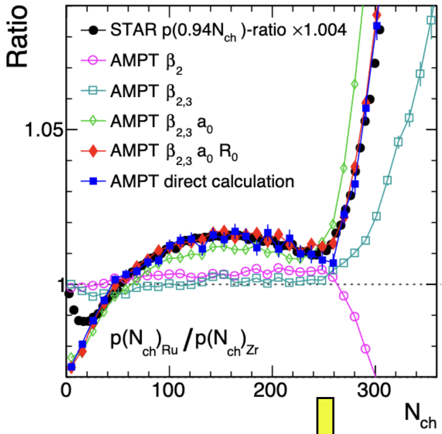

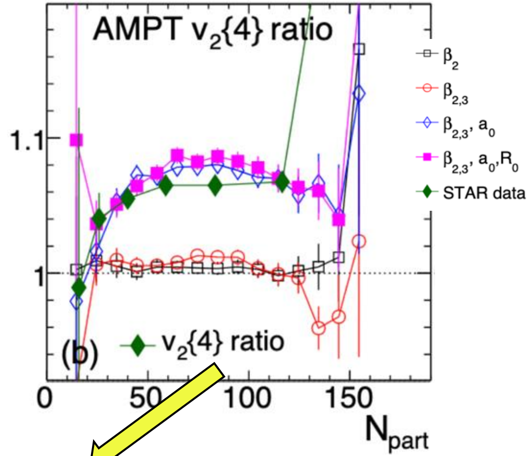

Constrain neutron skin and symmetry energy

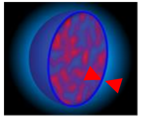

R_n-R_p

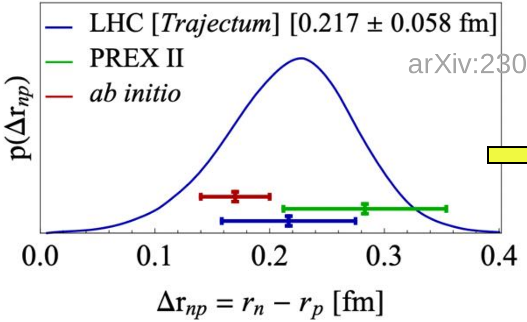

arXiv:2305.00015

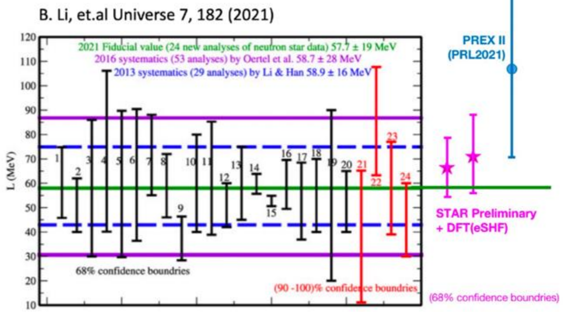

Summary

- Imaging-by-smashing is a discovery tool for low- and high-energy nuclear physics.
- Low- and high-energy techniques together enable study of evolution of nuclear structure across energy and time scales.
- Future research should conduct collider experiments with selected isobaric pairs

2102.08158

A	isobars	A	isobars	A	isobars	A	isobars	A	isobars	A	isobars
36	Ar, S	80	Se, Kr	106	Pd, Cd	124	Sn, Te, Xe	148	Nd, Sm	174	Yb, Hf
40	Ca, Ar	84	Kr, Sr, Mo	108	Pd, Cd	126	Te, Xe	150	Nd, Sm	176	Yb, Lu, Hf
46	Ca, Ti	86	Kr, Sr	110	Pd, Cd	128	Te, Xe	152	Sm, Gd	180	Hf, W
48	Ca, Ti	87	Rb, Sr	112	Cd, Sn	130	Te, Xe, Ba	154	Sm, Gd	184	W, Os
50	Ti, V, Cr	92	Zr, Nb, Mo	113	Cd, In	132	Xe, Ba	156	Gd,Dy	186	W, Os
54	Cr, Fe	94	Zr, Mo	114	Cd, Sn	134	Xe, Ba	158	Gd,Dy	187	Re, Os
64	Ni, Zn	96	Zr, Mo, Ru	115	In, Sn	136	Xe, Ba, Ce	160	Gd,Dy	190	Os, Pt
70	Zn, Ge	98	Mo, Ru	116	Cd, Sn	138	Ba, La, Ce	162	Dy,Er	192	Os, Pt
74	Ge, Se	100	Mo, Ru	120	Sn, Te	142	Ce, Nd	164	Dy,Er	196	Pt, Hg
76	Ge, Se	102	Ru, Pd	122	Sn, Te	144	Nd, Sm	168	Er,Yb	198	Pt, Hg
78	Se, Kr	104	Ru, Pd	123	Sb, Te	146	Nd, Sm	170	Er,Yb	204	Hg, Pb

Shape Coexistence Workshop - 2023